

Investigation of a Wind Power Generator

Part 1

Ingemar Mathiasson

November 2005

Department for Energy and Environment

Division of Electric Power Engineering

Chalmers University of Technology

CONTENTS

1	INTRODUCTION	3
2	ABOUT FEM CALCULATIONS	4
2.1	GENERAL	4
2.2	THE SPECIFIC ELECTROMAGNETIC PROBLEM	4
3	FEM-ANALYSIS APPLIED ON THE GENERATOR	7
4	SIMULATION RESULTS BASED ON FEM-ANALYSIS.....	13
4.1	VOLTAGE – CURRENT-SIMULATIONS	13
4.1.1	<i>Basics</i>	13
4.1.2	<i>No load calculations</i>	16
4.1.3	<i>Load calculations</i>	16
4.2	DEMAGNETIZATION CURRENT.....	20
4.3	COIL INDUCTANCE	26
4.4	THE STATOR COIL WIRING NUMBER	29
4.5	THE AIRGAP BETWEEN ROTOR AND STATOR	30
5	FOURIER ANALYSIS REGARDING THE FLUX LINKAGE	34
5.1	GENERAL	34
5.2	GENERAL ABOUT DISCRETE FOURIER TRANSFORMING	34
5.3	D F T APPLIED ON THE FEM RESULT	36
5.4	CONCLUSION	40
6	FUTURE WORK.....	41
7	REFERENCES	42
APPENDIX	(USED SOFTWARE)	42

1 INTRODUCTION

The following work is Part 1 of a study regarding a technical investigation of the wind power system at Hönö (Hönö 3, generator Morley 27/48/1). The work has different goals:

- To increase the theoretical knowledge about some important electromagnetic phenomena e.g. demagnetization, the airgap dependence, the harmonic properties of the coil current and the coil inductance
- To evaluate possibilities of increasing the active power by increasing the coil current

The work has been performed around an analysis of the PM-generator in question, where one of the important methods has been FEM-analysis. The following main parts are included in this paper:

- General about the Finite Element Method (FEM) calculations
- FEM-analysis applied on the generator
- Simulation results based on FEM-analysis
 - Voltage – Current-simulations
 - Demagnetization current
 - Coil inductance
 - The stator coil wiring number
 - The airgap between rotor and stator
- Fourier analysis regarding the flux linkage
 - General about discrete fourier transforming
 - Dft applied on the FEM result

Part 2 of this study ([1]) deals with the question about the reactive effect compensation.

2 ABOUT FEM CALCULATIONS

2.1 General

The Finite Element Method is a numerical analysis method for solving (partial) differential equations. The method is very useful in combination with complex geometry. The geometry in question is here divided into a mesh of elements consisting of triangles in 2D and tetrahedrons in 3D. The analysis is then performed separately for every single element. The result of this analysis is modeled as polynomials (one polynomial for each element) in the spatial coordinates (e.g. x, y). The finite element analysis is the solution of the set of equations for the unknown coefficients in all polynomials. By a system analysis the results from the single elements is adapted into a total system solution. This is done by matching the results of adjacent elements to each other (e.g. connect adjacent element to each other).

2.2 The specific electromagnetic problem

One important field for FEM is to solve electromagnetic problems. In this case it is of interest to solve problems in the low frequency region. This is when the electromagnetic wavelength ($\lambda = c/f$) is much larger than the geometrical dimensions.

Maxwell's equations could be stated according to the following:

$$\text{(Equation 1)} \quad \nabla \times H = J + \frac{\partial D}{\partial t} \quad \text{(Ampère's law)}$$

$$\text{(Equation 2)} \quad \nabla \times E = -\frac{\partial B}{\partial t} \quad \text{(Faraday's law)}$$

$$\text{(Equation 3)} \quad \nabla \cdot D = \rho \quad \text{(Poisson's equation)}$$

$$\text{(Equation 4)} \quad \nabla \cdot B = 0 \quad \text{(The condition of solenoid magnetic field)}$$

H : the magnetic field intensity (A/m)

J : current density (A/m²)

D : electric flux density (As/m²)

E : the electric field (V/m)

B : the magnetic flux density (Vs/m²)

ρ : charge density (As/m³)

The following relations are available:

$$\begin{aligned} \text{(Equation 5, Equation 6)} \quad B &= \mu \cdot H \\ D &= \varepsilon \cdot E \end{aligned}$$

μ is the material's magnetic permeability and ε is the coefficient of dielectricity. As the magnetic permeability μ for ferromagnetic materials usually is dependent on the magnetic flux density it is in this case a nonlinear problem to solve.

In this case the low frequency approximation is in question. This approximation implies that $\varepsilon = 0$ and the displacement current in Ampère's law could be neglected. In the FEM-calculation the magnetostatic case is assumed and take use of the following equations:

$$\begin{aligned} \text{(Equation 7, Equation 8)} \quad \nabla \times H &= J \\ \nabla \cdot B &= 0 \end{aligned}$$

Since $\nabla \cdot B = 0$ there exists a magnetic vector potential \mathbf{A} such that

$$\text{(Equation 9)} \quad B = \nabla \times A$$

and

$$\text{(Equation 10)} \quad \nabla \times \left(\frac{1}{\mu} \nabla \times A \right) = J$$

As the plane case (2D) is in question the current flows are parallel to the z-axis and only the z component of \mathbf{A} is present:

$\mathbf{A} = (0,0,A)$ and $\mathbf{J} = (0,0,J)$ and the equation can be simplified to the following elliptic partial differential equation

$$\text{(Equation 11)} \quad -\nabla \cdot \left(\frac{1}{\mu} \nabla A \right) = J$$

where $J = J(x,y)$.

$$\text{(Equation 12)} \quad \nabla \cdot \left(\frac{1}{\mu} \nabla A \right) = \frac{1}{\mu} \left(\frac{\partial^2 A}{\partial x^2} + \frac{\partial^2 A}{\partial y^2} \right)$$

and

$$\text{(Equation 13)} \quad \frac{\partial^2 A}{\partial x^2} + \frac{\partial^2 A}{\partial y^2} = \mu \cdot J(x, y)$$

Then the magnetic flux density B could be computed as

$$\text{(Equation 14)} \quad B = \left(\frac{\partial A}{\partial y}, -\frac{\partial A}{\partial x}, 0 \right)$$

The magnetic field intensity H is given by

$$\text{(Equation 15)} \quad H = \frac{1}{\mu} B$$

The interface condition between regions of different material properties is that $H \times n$ should be continuous. This implies the continuity of

$$\frac{1}{\mu} \frac{\partial A}{\partial n}$$

The magnetostatic potential A is on the boundary specified by the Dirichlet boundary condition.

The value on the boundary of the normal component of

$$n \left(\frac{1}{\mu} \nabla A \right)$$

is specified by the Neumann condition. This is equivalent to specify the tangential value of the magnetic field H on the boundary.

When solving the present problem the magnetostatic potential A is calculated for every single triangle (defined by the mesh of elements consisting of triangles). As mentioned in chapter 2.1 the result of this analysis is modeled as polynomials. The finite element analysis is then the solution of the set of equations for the unknown coefficients in all polynomials followed by an adaption into a total system solution where adjacent elements are adapted to each other.

3 FEM-ANALYSIS APPLIED ON THE GENERATOR

A first study of the generator is presented in [1].

The configuration of the device is shown in Figure 1. The first approximation will be to handle the device as a symmetric construction. This is not quite correct (there are 24×2 rotor poles and 27 stator E-cores). It is important to remember this approximation when using the model. This approximation makes it for example impossible to study the field in more than **one** stator E-core at the same time (same rotor position), and to compare the results).

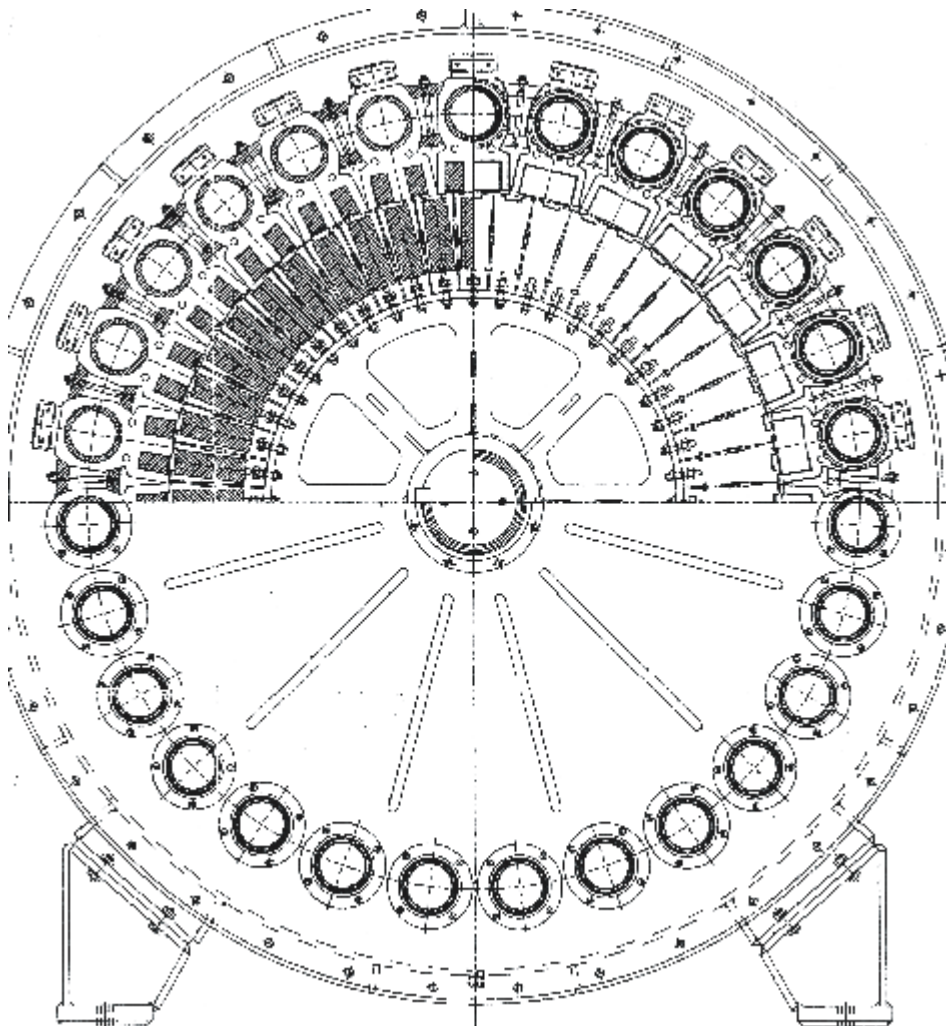


Figure 1 Configuration of the studied PM-generator consisting of 27 stator modules and 24×2 rotor poles

Figure 2 gives more in detail the configuration of the stator and rotor modules. From a circular geometry the configuration then is approximated into a rectangular geometry according to Figure 3.

The FEM-calculations have been performed by a software named “Magnet” from Infolytica Corporation. Two examples of used geometries are illustrated in Figure 4 and Figure 5. These figures correspond to different relative positions between the stator module and the rotor module. This is named “X-shift” in the figures. By calculating the coil flux linkage for different X-shift we get information about the coil flux linkage as a function of rotor position. This give us on the other hand a possibility to calculate the time derivative of the coil flux linkage and hereby the induced voltage for a given rotating speed of the generator. Figure 6 illustrates a part of the model and Figure 7 gives the corresponding flux image.

By using the method of “shifting” the stator – rotor position we have a possibility to calculate the coil inductance as a function of position.

The following points are discussed in [1] and are not treated in this paper:

- Different geometric configurations
- Air-box sizes
- Solution polynom orders
- Mesh sizes

The following main points have been treated regarding FEM-analysis:

- Voltage – Current-simulations
- Demagnetization current
- Coil inductance
- Determination of the stator coil wiring number
- The airgap between rotor and stator

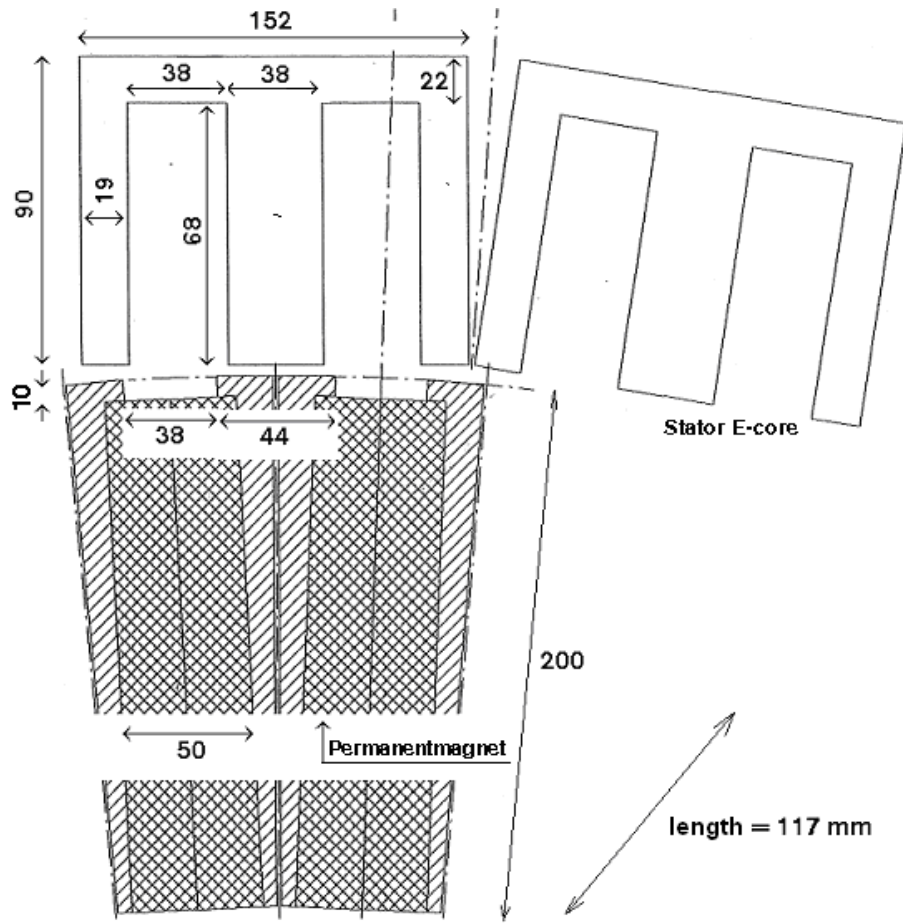


Figure 2 The stator- and rotor modules. Dimensions in mm. In the FEM-calculations we have used the following material:

- Permanent magnet: Ceramic ferrite
B-Max: 0.4 Wb, Hc: $-2.7 \cdot 10^5$ A/m
- Other components: Cold rolled 1010 steel
B-Max: 2.15 Wb, Hc: 0

The distance between two equivalent points of stator modules is assumed to 164 mm. See Figure 3.

The airgap between rotor and stator is 2 mm, nominal value. See chapter 4.5.

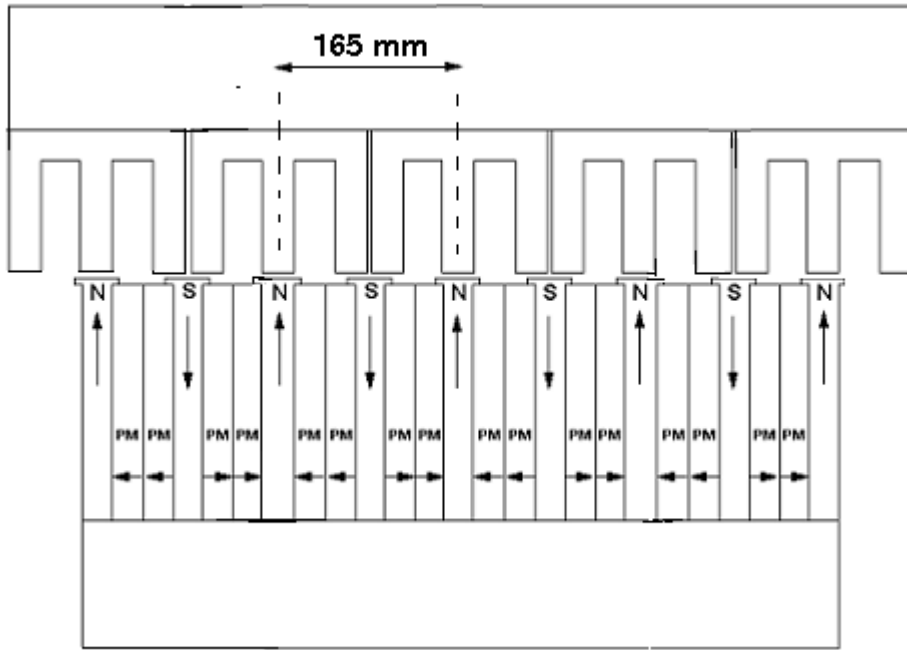


Figure 3 Model configuration for 9 poles in combination with 5 E-cores. The figure illustrates the magnetic flow direction in the rotor parts. The distance between two equivalent points of stator modules is assumed to 165 mm

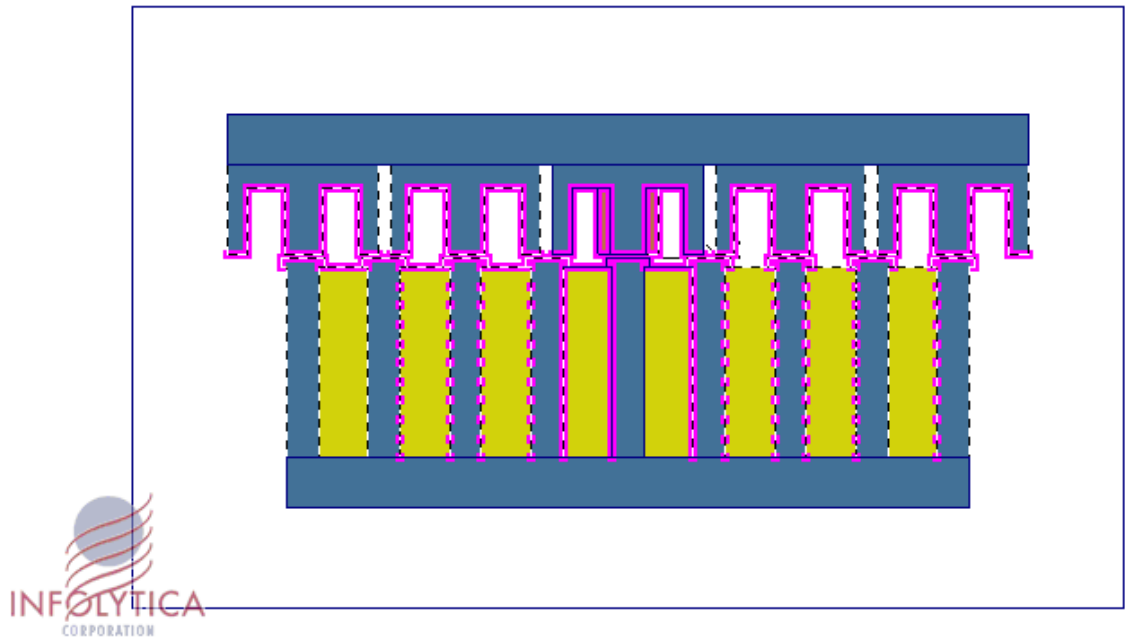


Figure 4 Geometric model used for the FEM-calculations. X-shift 0 mm

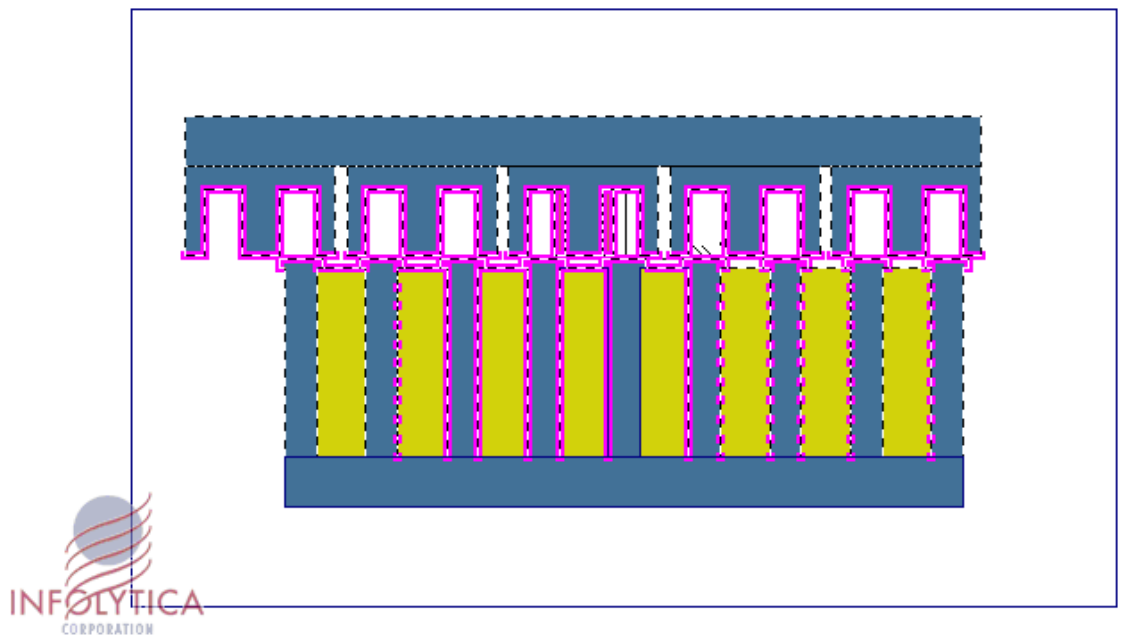


Figure 5 Geometric model used for the FEM-calculations. X-shift in this example 41 mm

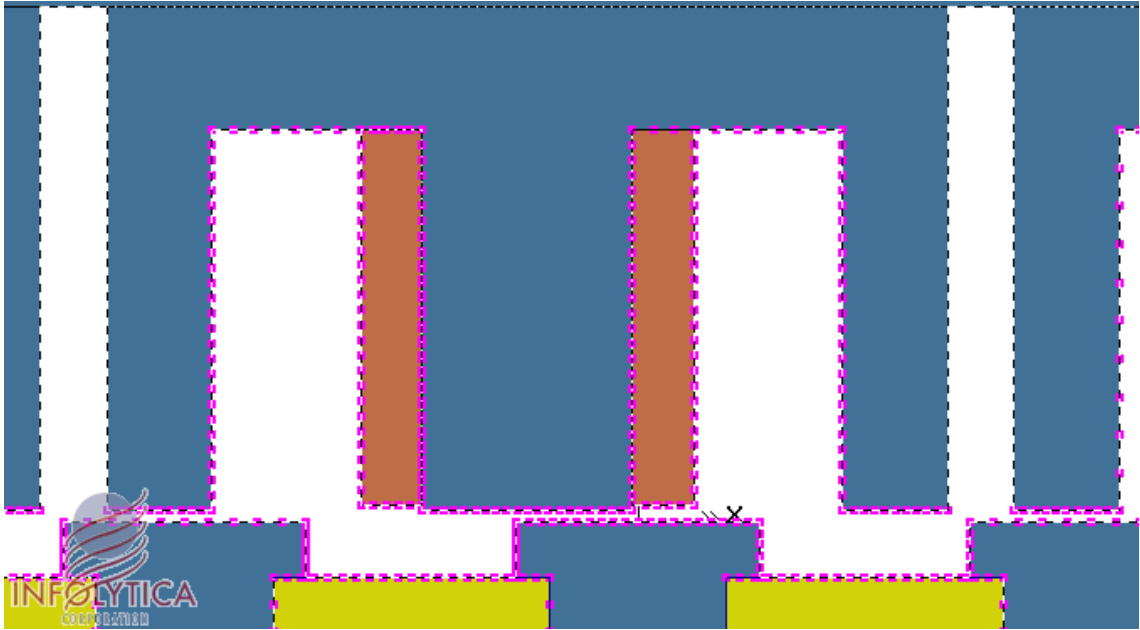


Figure 6 Part of the geometric model. X-shift in this example 20 mm. The coil is wired around the middle E-core

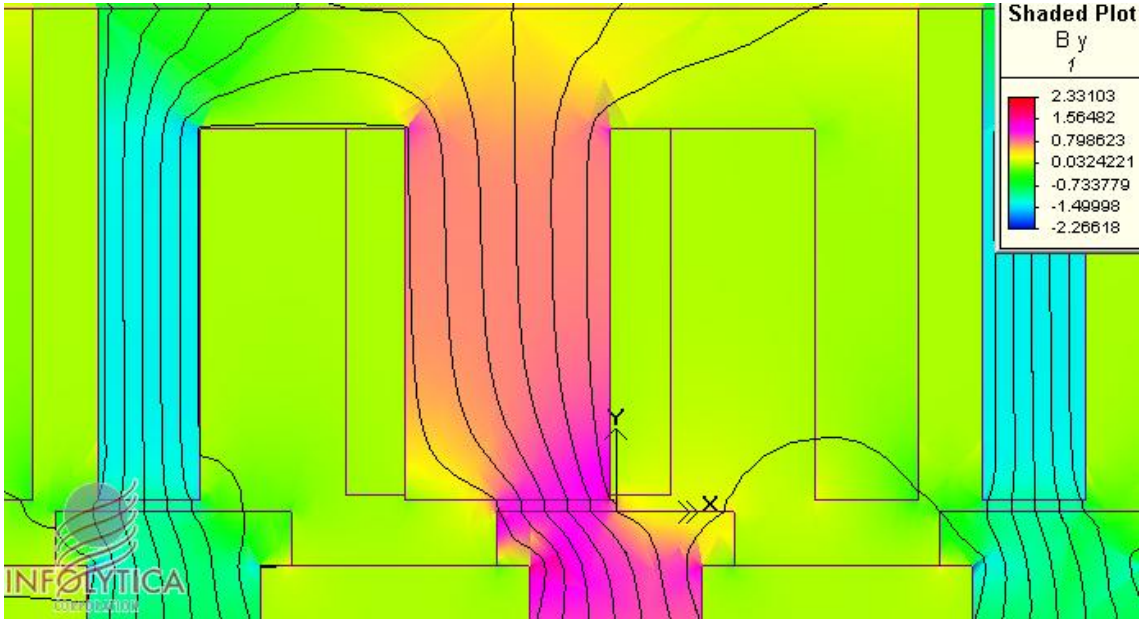


Figure 7 Calculated flux image corresponding to Figure 6

4 SIMULATION RESULTS BASED ON FEM-ANALYSIS

4.1 Voltage – Current-simulations

4.1.1 Basics

In **Table 1** we have the calculated flux linkage values for a coil with 323 turns. No current in the coil.

Shiftposition (mm)	Flux linkage (Weber)
0	-1.57463
2.5	-1.56709
5	-1.54017
7.5	-1.49872
10	-1.44704
12.5	-1.38729
15	-1.31946
17.5	-1.25001
20	-1.1811
22.5	-1.11004
25	-1.03145
27.5	-0.93993
30	-0.82634
32.5	-0.68853
35	-0.51895
37.5	-0.32085
40	-0.10013
42.5	-0.00646
45	0.134045
47.5	0.350455
50	0.543717
52.5	0.705755
55	0.837647
57.5	0.944775
60	1.031985
62.5	1.108428
65	1.177873
67.5	1.245703
70	1.315687
72.5	1.381902
75	1.440042
77.5	1.489568
80	1.528867
82.5	1.550938

Table 1 Flux linkage as a function of shift position. No current in the coil

As the distance between two equivalent points of stator modules is assumed to 165 mm we have a symmetry around a shift of 82.5 mm, $165\text{mm} + 82.5\text{mm}$, $2 \times 165\text{mm} + 82.5\text{mm}$,, and so on.

Figure 8 is a plot of how the flux linkage varies when the shift is alternated.

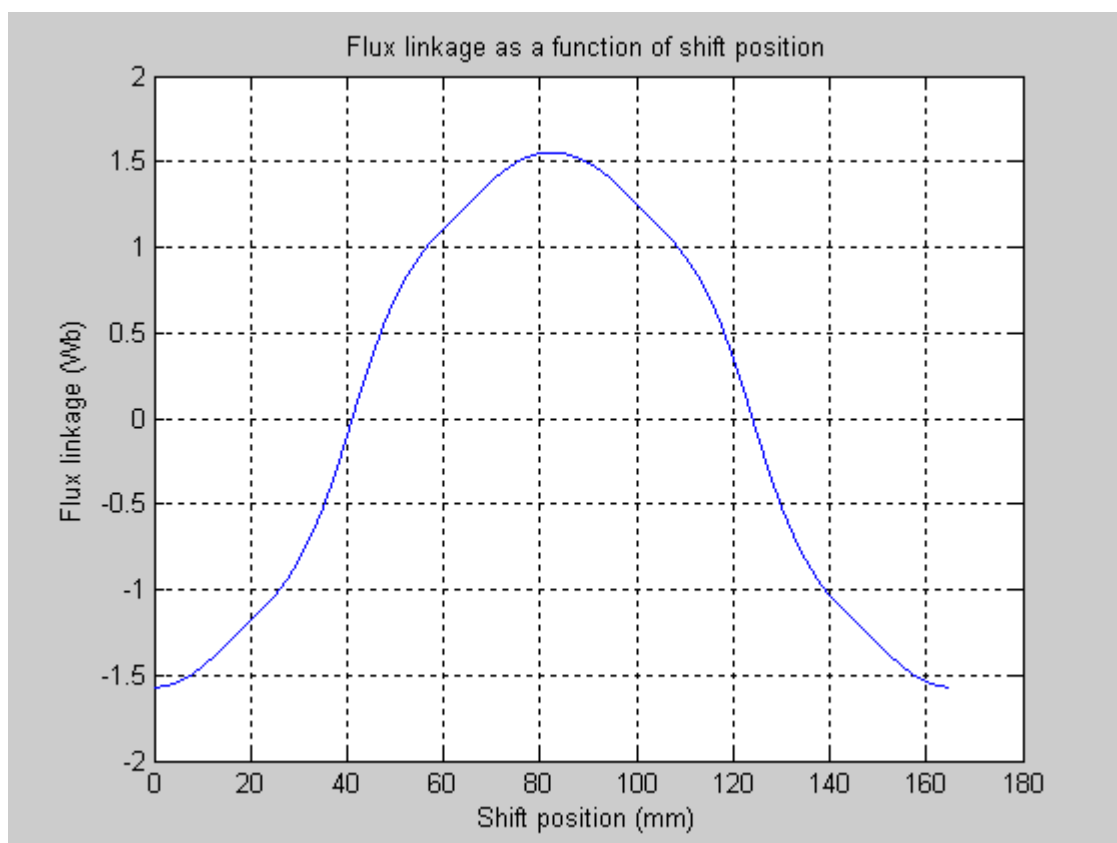


Figure 8 Flux linkage for a coil of 323 turns vs shift position

The position dependent flux linkage according to Figure 8 could be divided into a DC-component, a fundamental frequency and a number of harmonics. This is done in chapter 5. The analysis point out the fairness to approximate the flux variation with a single sinusoidal function based on the fundamental frequency. This results in a simple expression for the corresponding induced voltage in the coil if we suppose a flux linkage variation as a result of ordinary relative movement between the rotor and the stator. Suppose the following generator parameters:

A: amplitude of the fundamental regarding flux linkage (Wb)

V_{rot} : generator rotating speed (rpm)

P: number of pole pairs in the rotor

$\phi(t)$: flux linkage (Wb)

$u(t)$: induced voltage in the coil (V)

$$\text{(Equation 16)} \quad \phi(t) = A \cdot \sin\left(\frac{V_{rot} \cdot P}{60} 2\pi \cdot t\right)$$

$$\text{(Equation 17)} \quad u(t) = (-) \frac{d\phi(t)}{dt} = (-) A \cdot \frac{V_{rot} \cdot P}{60} 2\pi \cdot \cos\left(\frac{V_{rot} \cdot P}{60} 2\pi \cdot t\right)$$

Figure 9 gives the equivalent electrical circuit of a single stator module.

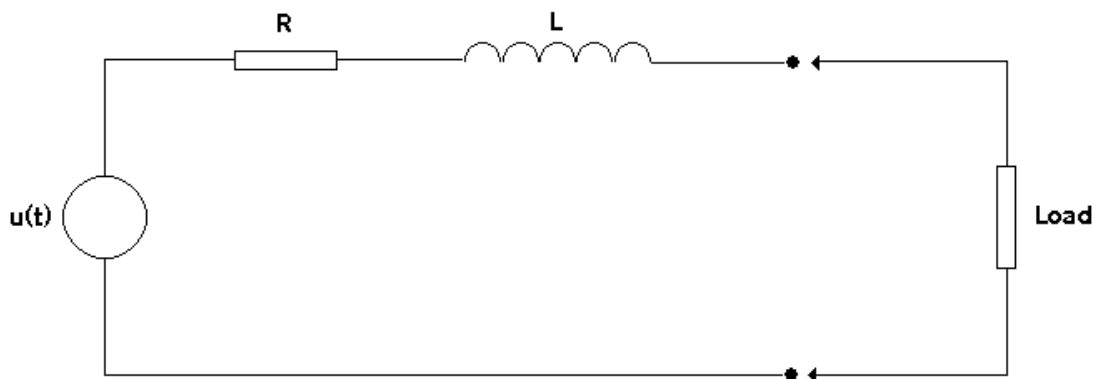


Figure 9 Equivalent circuit of the stator module

R: the coil resistance (Ω)

L: the coil inductance (H)

R and L have been measured to:

$R = 1.0 \Omega$ (20 °C)

$L = 106 \text{ mH}$ (mean value 20 °C)

$P = 24$

The fundamental amplitude A (based on FEM-calculations according to the above and fourier analysis according to chapter 5.3) = 1.615 Wb

4.1.2 No load calculations

Table 2 gives some examples of no load voltages (RMS), calculated by **(Equation 17,** for a stator module when the rotor speed is varied:

Rotor speed (rpm)	No load voltage, RMS (V)
50	144
70	201
80	230

Table 2 Some examples of no load voltages (RMS) for the stator module for different rotating speeds

4.1.3 Load calculations

To calculate load currents and load voltages we have used a special kind of simulation tool called “PLECS” (Piecewise Linear Electrical Circuit Simulation). The circuit according to Figure 10 corresponds to the circuit in Figure 9 with a load consisting of the ordinary “load circuit” (capacitor (C2) for reactive power compensation, diode bridge (D1 – D4), capacitor (C1) in parallel with a resistor (R1) representing the loaded DC-AC converter) for a stator module.

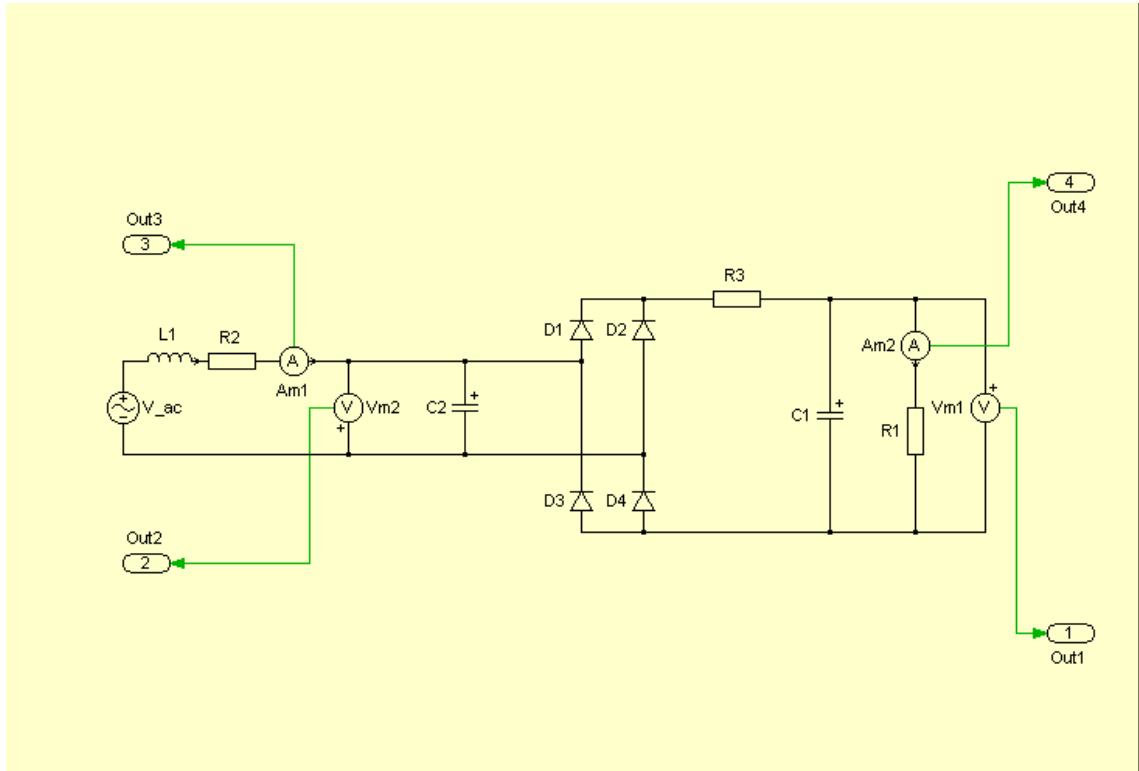


Figure 10 Used PLECS circuit for simulation

Different measurement campaigns have been realised. One of these is presented in [2]. Figure 11 and Figure 12 show some results from these measurements.

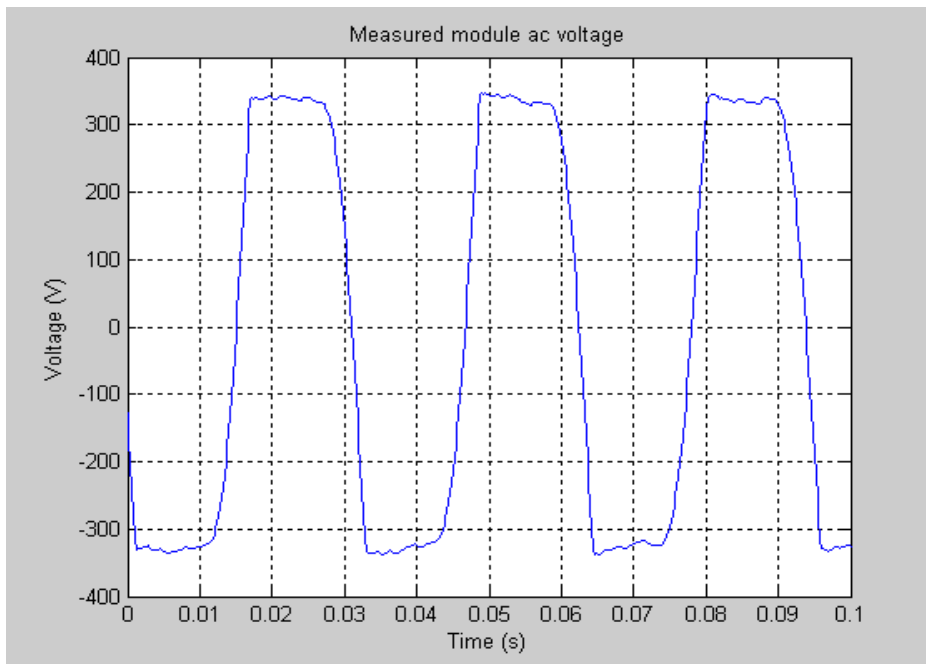


Figure 11 Measured module voltage

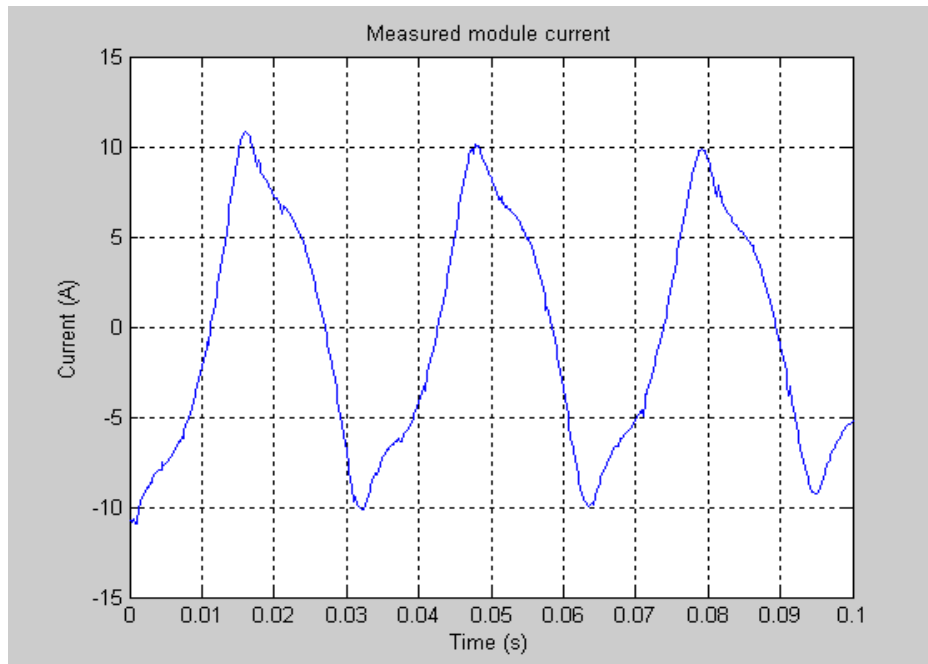


Figure 12 Measured module current

Measured module voltage and module current according to Figure 11 and Figure 12 is based on:

- Rotor speed: 80 rpm
- Generated power 20 kW/27 per module

If we use these parameters for simulation we get the results according to Figure 13 and Figure 14.

The other parameters are (referring to Figure 10):

V _{ac} :	$325 \cdot \cos(2\pi \cdot 32 t)$
L1:	106 mH
R2:	1 Ω
C2:	60 μF
D1 – D4:	forward voltage: 0V, on resistance: 0 Ω
R3:	0.1 Ω
C1:	1000 μF
R1:	200 Ω

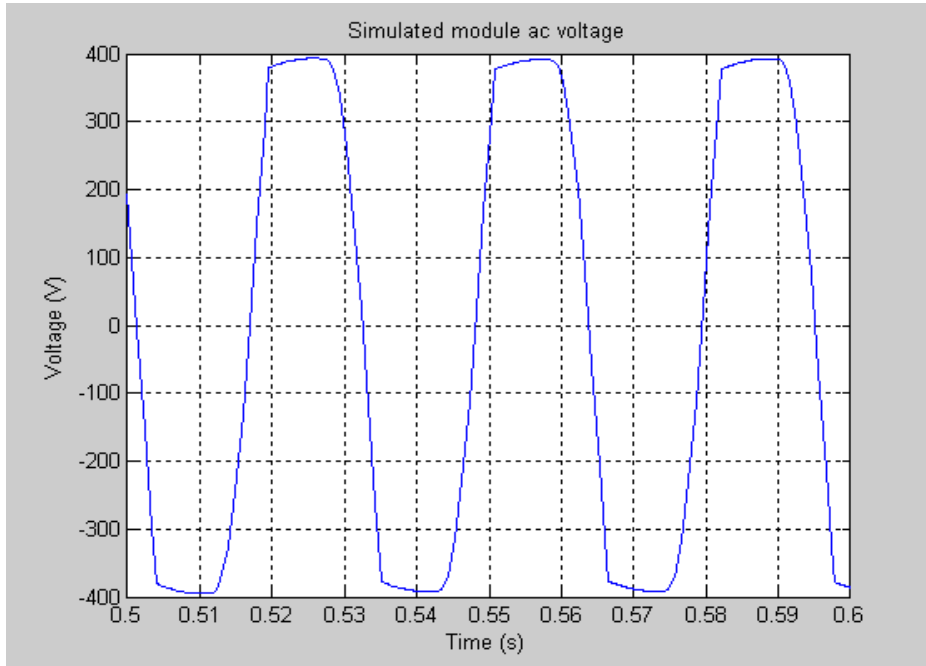


Figure 13 Simulated module voltage

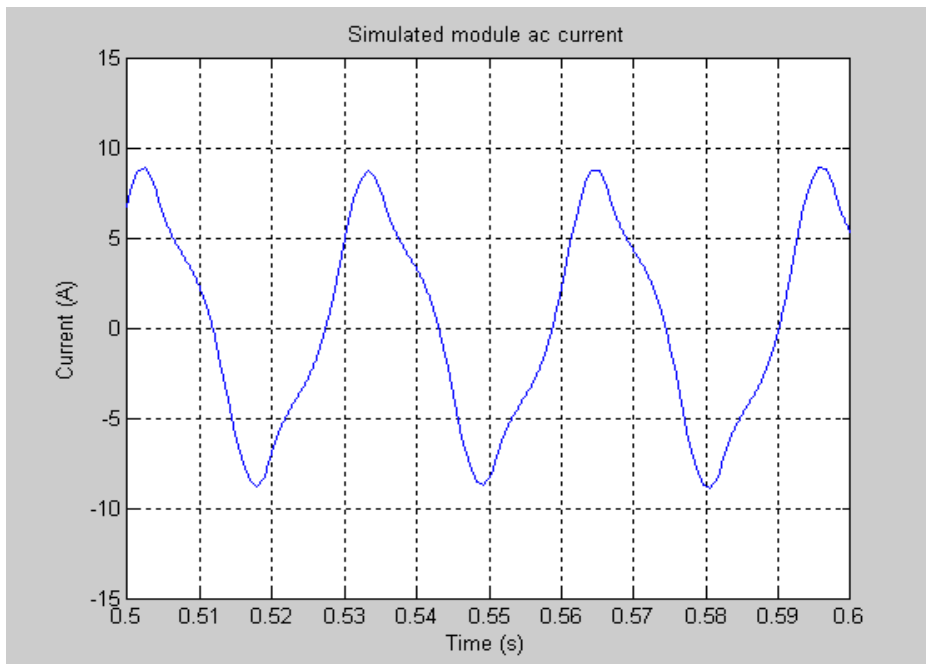


Figure 14 Simulated module current

When comparing Figure 11 (measured voltage) with Figure 13 (simulated voltage) it could be noted that the curve shapes are rather similar. The same similarity is on hand when comparing Figure 12 (measured current) with Figure 14 (simulated current). A corresponding comparison regarding the levels in question will give a **voltage difference** of about 14% **higher** top level for the simulated case compared with the measured one and a **current difference** of about 20 % **lower** top level for the simulated case compared with the measured one. However, as there are some uncertainties regarding some, for the result important, parameter values, that have been estimated, we can not expect a better agreement between simulated and measured results. There are especially two parameters that for the moment are sources for uncertainties; the coil inductance and the air gap. These parameters are treated in points 4.3, 4.4 and 4.5. See also point 6 for some suggestions of future works.

4.2 Demagnetization current

If a permanent magnet is exposed to an external magnetic field that is reversed to its own direction there is a risk for reduction of the permanent magnet capacity. Figure 15 gives an example of a part of a B-H characteristic for a certain permanent magnet. B_r corresponds to the remanence flux density and H_c is the coercivity. Suppose that a magnetic field intensity of H_1 is applied to the permanent magnet. The corresponding flux density will be B_1 . If H_1 then is reduced to zero the resulting flux density in the **general case** will follow a line called the “recoil line”. That means that, for the general case, we can't expect to return to the original remanence flux density, B_r , but another one, some reduced, in the figure called B_r' . In this example we have got a partial demagnetization of the permanent magnet. The size of this demagnetization depends on the material in question and on the size of the reversed magnetic field. In “the Hönö generator” there is a similar situation. In this case the permanent magnets are exposed to the reversed magnetic fields from the stator poles. The size of the reversed field depends on the size of the coil current. Supposing that a reversed field on the permanent magnet, to some extent, will cause a reduction of the remanence there is a necessity to find a limit of the coil current that is well adjusted to the induced voltage (some reduced as an effect of the remanence decreasing) in order to get an optimal total power. Relating to Figure 15, there is somewhere in between the zero point and the point corresponding to the coercivity, an optimal point resulting in an acceptable demagnetization, regarding the maximum available power. This point is marked as point 2 in Figure 15. In the case of “the Hönö generator” there is, for the moment, no information available to give a possibility to with certainty calculate the location of point 2 (the optimal point). We make temporarily the assumption that the optimal point is located somewhere in the region near the coercivity force. That imply a simple way to estimate the largest current that could be flowing in a coil without risk to seriously reduce the capacity of the permanent magnet by demagnetization. The method is to calculate the current that results in a flux that exactly balance the permanent magnet flux in the airgap. For larger currents the permanent magnet get fluxes in reversed direction with risk for seriously capacity reduction.

Figure 16 - Figure 18 illustrate the flux images with different coil currents. For a coil current of about 17 A the flux in the airgap is zero. If the current exceeds this limit the resulting flux will get a direction that is reversed to the permanent magnet.

According to this calculation we draw the conclusion that the limit current for seriously demagnetization of the permanent magnets has an amplitude of less than 17 A. (i.e. an rms value of about 12 A).

As mentioned above there is in the writing moment lack of specific information regarding the permanent magnets and their magnetizing properties in respect of demagnetization. Therefore it is recommended that further studies will be performed in order to more in detail specify the maximum acceptable coil current.

In order to get a primarily value regarding a suitable limit for upper coil current it for the moment will be suggested a current value that results in a magnetic field intensity corresponding to 85 % of the coercivity force, H_c . This is the same as 85 % of 17 A, which is about **14.5 A**. This value is used in the analysis described in [3].

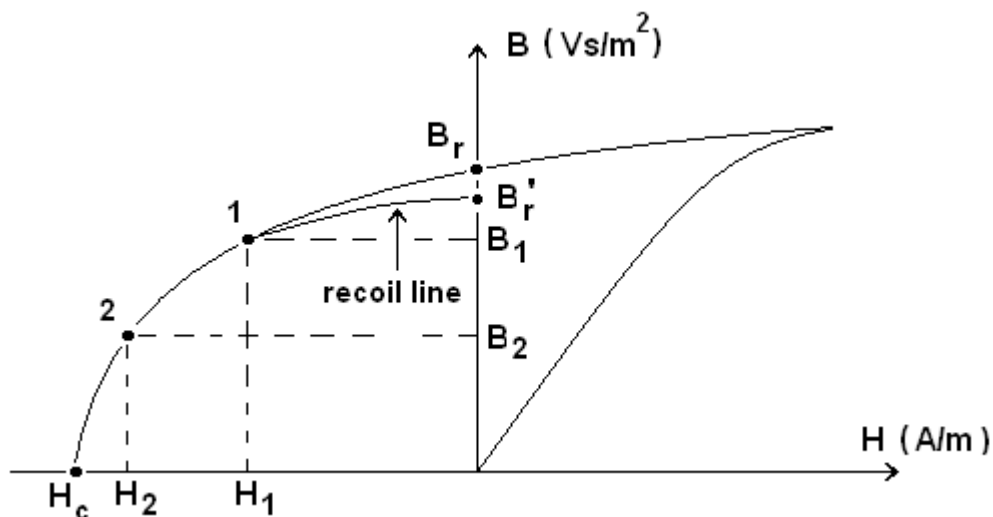


Figure 15 Portion of a B-H characteristic (example)

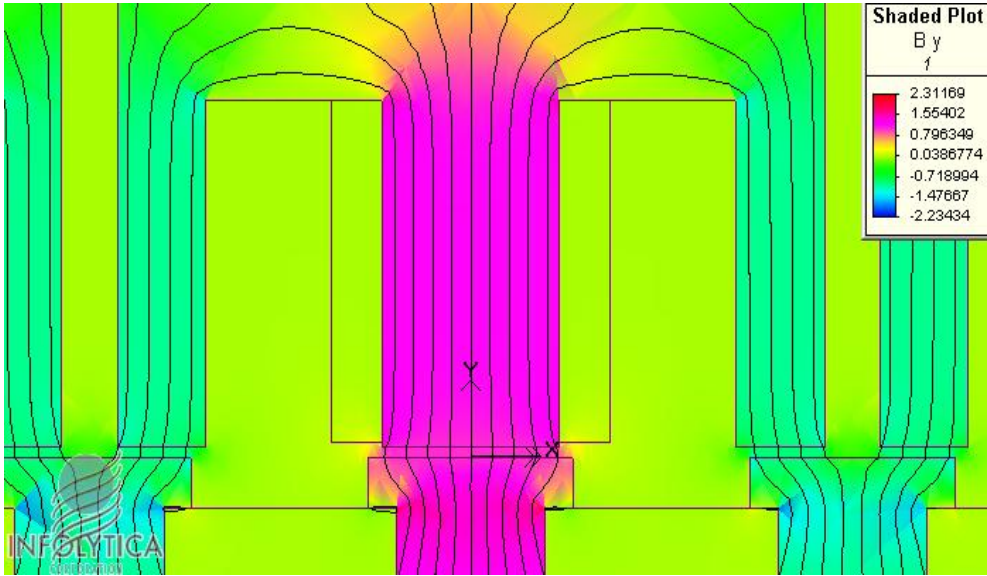


Figure 16 Flux image for a coil current of 0 A

Shaded Plot Field Line Graph

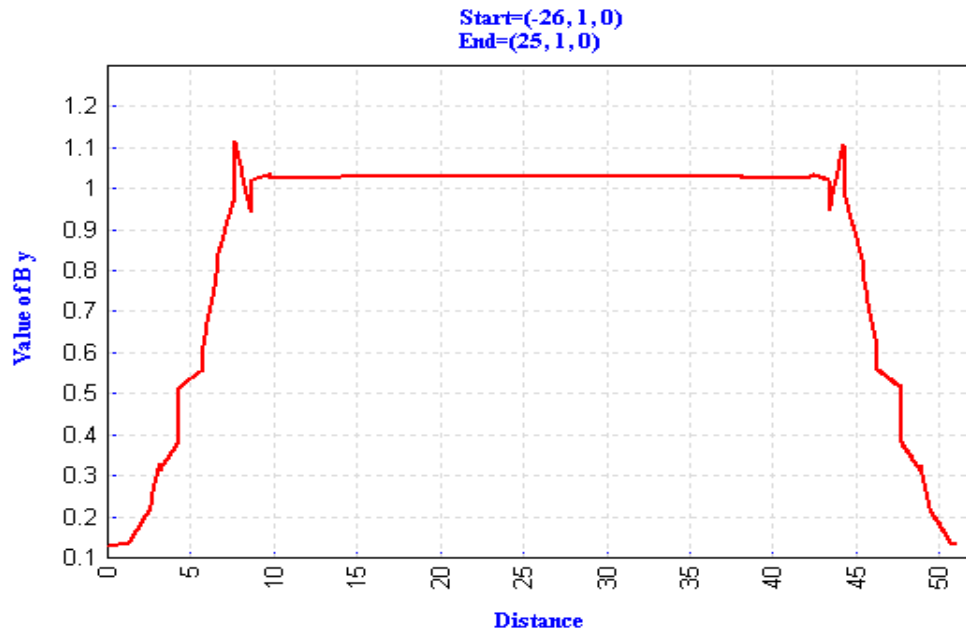


Figure 17 Airgap flux for a coil current of 0 A

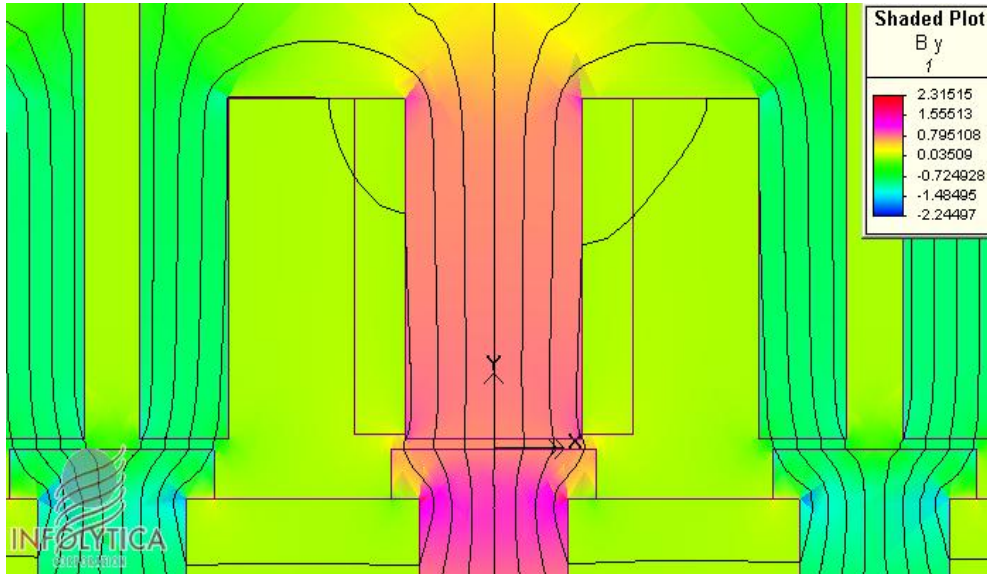


Figure 18 Flux image for a coil current of 5 A

Shaded Plot Field Line Graph

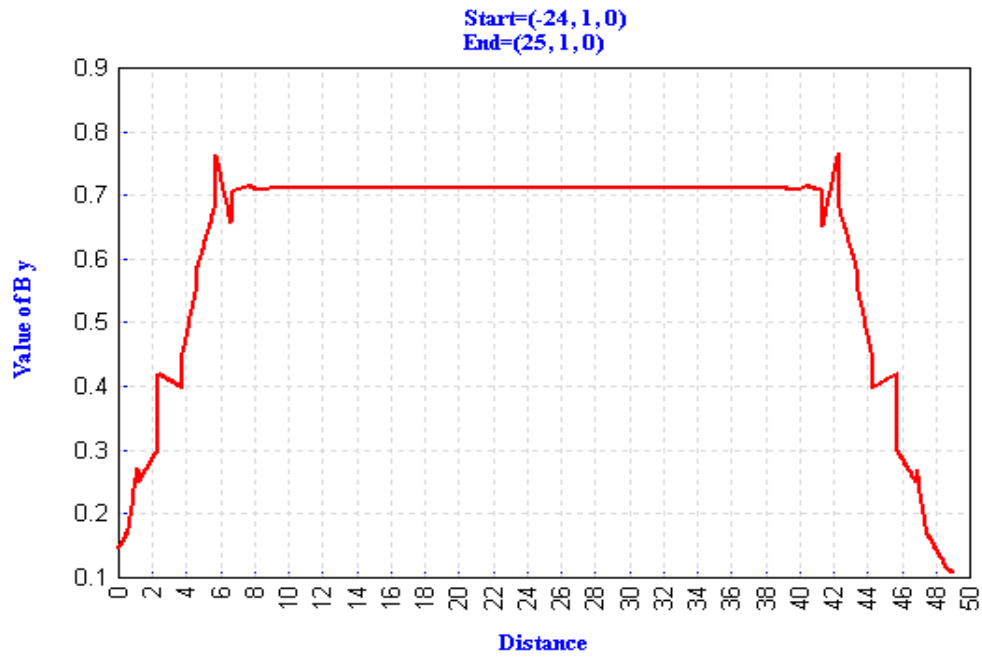


Figure 19 Airgap flux for a coil current of 5 A

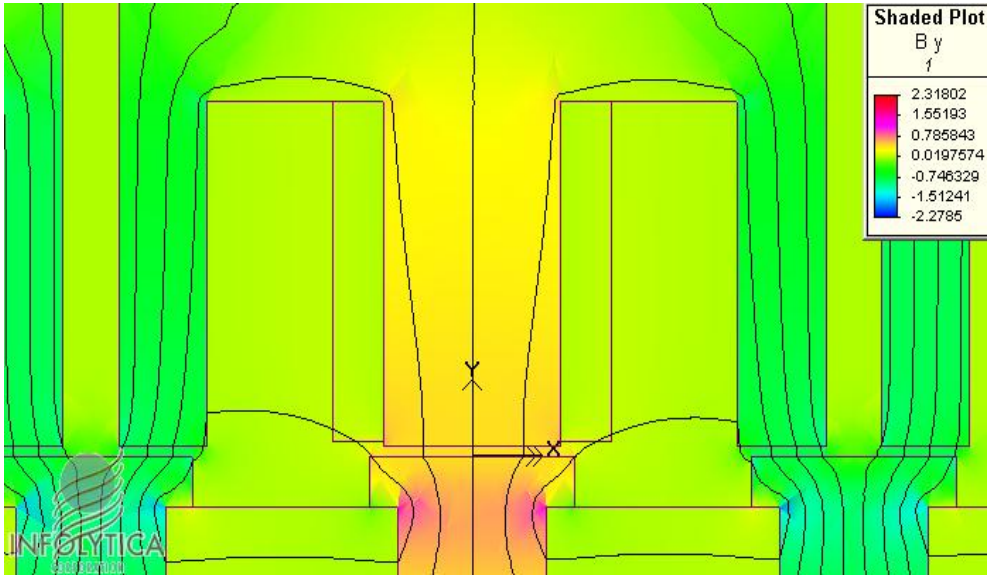


Figure 20 Flux image for a coil current of 10 A

Shaded Plot Field Line Graph

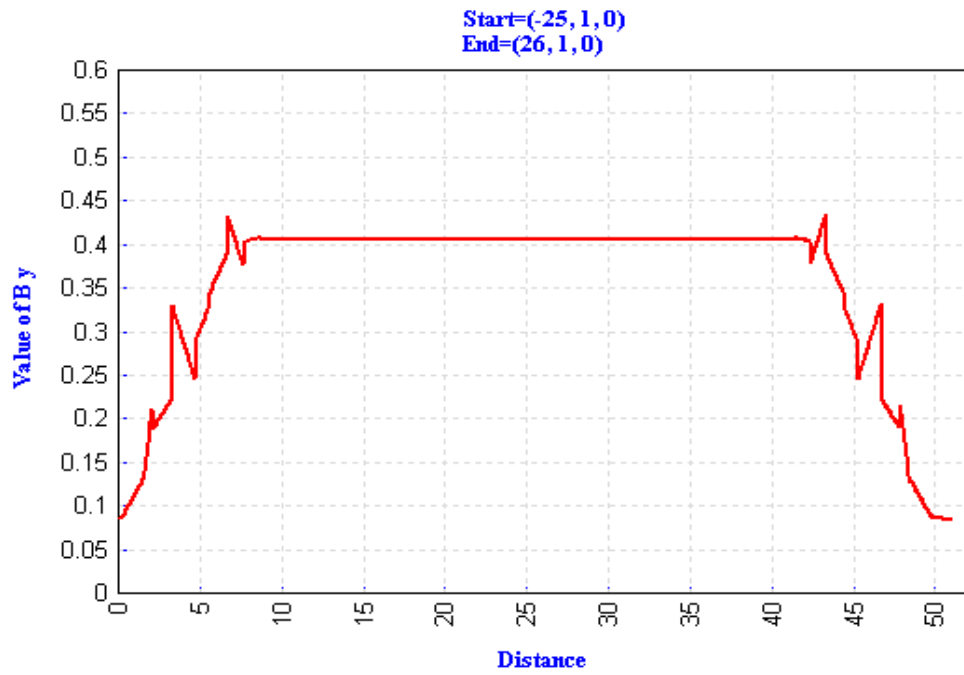


Figure 21 Airgap flux for a coil current of 10 A

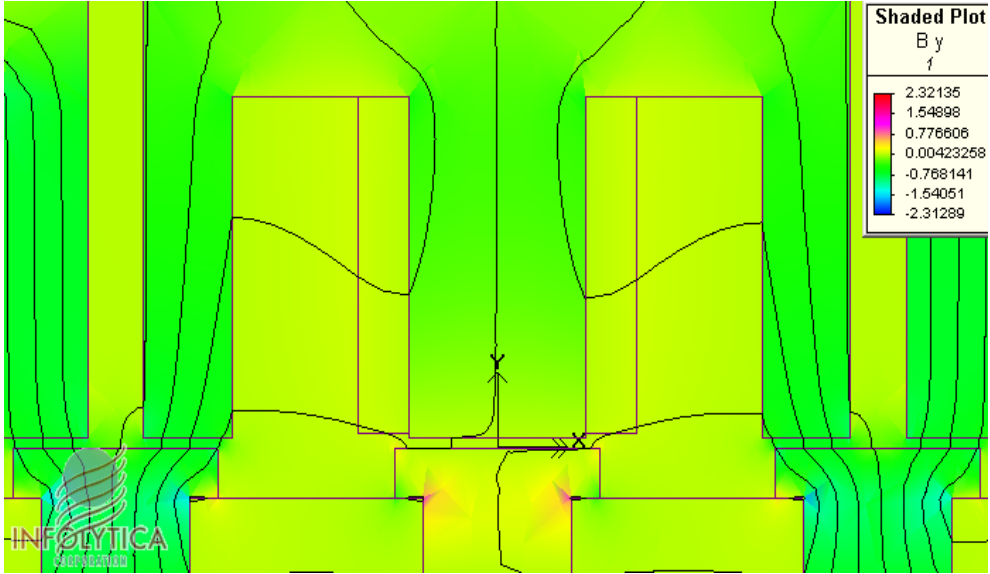


Figure 22 Flux image for a coil current of 17 A

Shaded Plot Field Line Graph

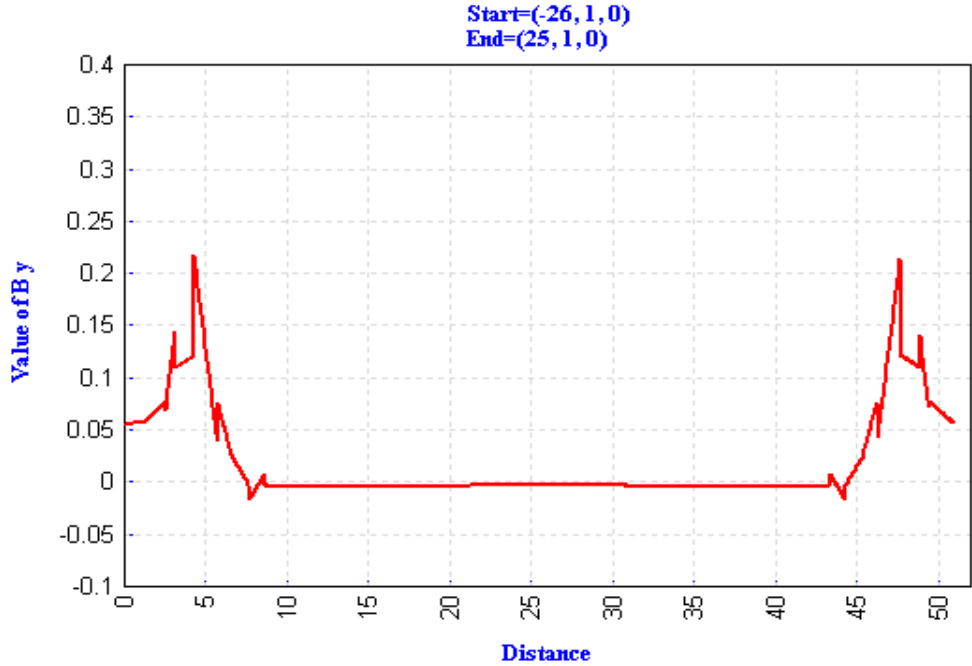


Figure 23 Airgap flux for a coil current of 17 A

4.3 Coil inductance

The coil inductance has been measured. This parameter depends on the relative position between stator and rotor. The inductance was randomly measured at different relative positions (40 positions randomly) between stator and rotor. The result was:

Mean value (measured): 106 mH

Max value (measured): 114 mH

Min value(measured): 99 mH

Total relative inductance variation $\frac{L_{\max} - L_{\min}}{L_{\text{mean}}}$ is about 14 %.

The standard deviation: 4 mH

The mean value 106 mH is used in the calculation above.

Table 3 gives the randomly measured values.

The coil inductance has been calculated as a function of relative position between stator and rotor. As the coil wiring number was unknown we had to estimate a reasonable value.

The first assumption, based on some data specifications of the generator, was that the coil wiring number was 600. This resulted in the values presented in Figure 24.

The principle for calculation was to calculate the flux linkage for two coil currents (+1 A and -1 A was used) and then use the definition of inductance according to the following expression: $L = \frac{\Delta\phi}{\Delta I}$, where $\Delta\phi$ is the flux linkage change for a coil current change of $\Delta I = 2$ A (a change between +1 A to -1 A).

Table 4 gives the calculated flux values for the two currents and 600 turns of the coil.

Random position	Measured inductance (H)	Random position	Measured inductance (H)	Random position	Measured inductance (H)	Random position	Measured inductance (H)
1	0.112835	11	0.101982	21	0.108047	31	0.111682
2	0.108362	12	0.100742	22	0.103926	32	0.108362
3	0.10423	13	0.102945	23	0.101037	33	0.099487
4	0.110553	14	0.101037	24	0.100401	34	0.100401
5	0.114011	15	0.105947	25	0.110553	35	0.110553
6	0.101982	16	0.103245	26	0.101982	36	0.10228
7	0.106986	17	0.100109	27	0.10228	37	0.107299
8	0.111357	18	0.103926	28	0.107299	38	0.10423
9	0.111357	19	0.102945	29	0.10228	39	0.109447
10	0.104927	20	0.103926	30	0.111682	40	0.105233

Table 3 Measured inductances for different randomly positions

Shiftposition (mm)	Flux linkage + 1 A (Weber)	Flux linkage - 1 A (Weber)	Shiftposition (mm)	Flux linkage + 1 A (Weber)	Flux linkage - 1 A (Weber)
0	-3.333	-2.517	85	2.472	3.289
2.5	-3.318	-2.503	87.5	2.433	3.247
5	-3.266	-2.455	90	2.363	3.169
7.5	-3.185	-2.382	92.5	2.276	3.072
10	-3.084	-2.291	95	2.174	2.958
12.5	-2.966	-2.185	97.5	2.058	2.827
15	-2.833	-2.067	100	1.935	2.689
17.5	-2.694	-1.944	102.5	1.816	2.552
20	-2.555	-1.824	105	1.694	2.411
22.5	-2.41	-1.699	107.5	1.559	2.257
25	-2.25	-1.561	110	1.405	2.082
27.5	-2.067	-1.398	112.5	1.212	1.874
30	-1.849	-1.194	115	0.972	1.626
32.5	-1.591	-0.942	117.5	0.675	1.324
35	-1.276	-0.631	120	0.321	0.965
37.5	-0.909	-0.269	122.5	-0.078	0.569
40	-0.507	0.142	125	-0.507	0.142
42.5	-0.078	0.569	127.5	-0.909	-0.269
45	0.321	0.965	130	-1.276	-0.631
47.5	0.675	1.324	132.5	-1.591	-0.942
50	0.972	1.626	135	-1.849	-1.194
52.5	1.212	1.874	137.5	-2.067	-1.398
55	1.405	2.082	140	-2.25	-1.561
57.5	1.559	2.257	142.5	-2.41	-1.699
60	1.694	2.411	145	-2.555	-1.824
62.5	1.816	2.552	147.5	-2.694	-1.944
65	1.935	2.689	150	-2.833	-2.067
67.5	2.058	2.827	152.5	-2.966	-2.185
70	2.174	2.958	155	-3.084	-2.291
72.5	2.276	3.072	157.5	-3.185	-2.382
75	2.363	3.169	160	-3.266	-2.455
77.5	2.433	3.247	162.5	-3.318	-2.503
80	2.472	3.289	165	-3.333	-2.517
82.5	2.48	3.298			

Table 4 Calculated flux linkage as a function of shift position and with current in the coil. Two current values was used: + 1 A and - 1 A. Coil wiring number = 600

interesting topic regarding a future work.

In the calculations according to 4.1 we have regarded the coil inductance as independent of the stator-rotor relative position. As the inductance has an influence on the resulting stator voltage, it could be a good idea to in the future, realize a more detailed analysis regarding the real effect of the inductance variation.

Regarding the coil inductance we consequently have the following topics for coming studies:

- investigation of inductance distribution (measurements and calculations)
- voltage dependent based on the inductance variation

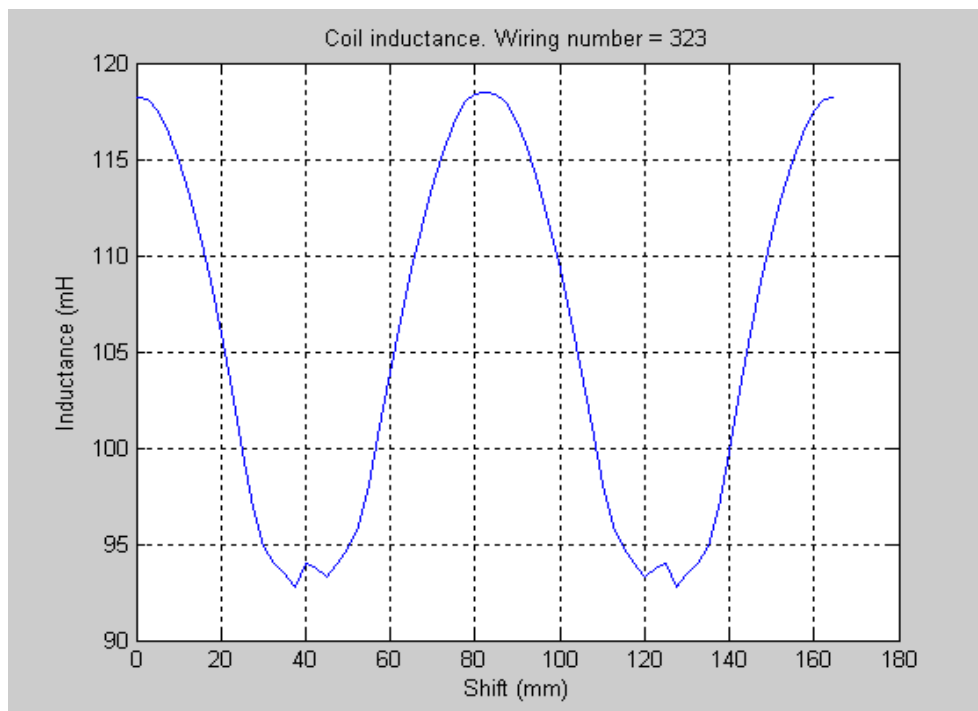


Figure 25 Corrected inductance values for a coil of 323 wiring numbers. The mean value of this inductances is 106 mH and agrees with the corresponding measured one

4.4 The stator coil wiring number

The stator coil wiring number has been estimated by using the measured coil inductance (106 mH) and the calculated coil inductance (see 4.3):

Measured coil inductance (mean value): 106 mH
 Calculated coil inductance (mean value) for a wiring number of 600: 365 mH

The coil inductance depends on the coil wiring number as:

$$L_1 / L_2 = (N_1 / N_2)^2$$

This give us the estimated wiring number as:

$$N_{\text{estimated}} = N_{L=365\text{mH}} \cdot (L_{\text{measured}} / L_{\text{calculated}})^{1/2}$$

$$N_{L=365\text{mH}} = 600 \quad L_{\text{measured}} = 106 \text{ mH} \quad L_{\text{calculated}} = 365 \text{ mH}$$

That will give us the estimated coil wiring number: 323 turns.

4.5 The airgap between rotor and stator

The airgap between rotor and stator has been assumed to 2 mm as a nominal value. As a result of mechanical imperfections this value varies during the rotation motion. This variation causes on the other hand a variation regarding the resulting flux linkage of the coil and thereby also a variation of the induced voltage. Figure 26 illustrates an example of measured “no load voltage and current” for the stator modules. The variation of the different modules is understood as an effect of varying airgap between stator and rotor vs rotor position. According to Figure 26 the following could be noted:

$$V_{\text{max}} = 268 \text{ V} \quad V_{\text{min}} = 249 \text{ V} \quad V_{\text{mean}} = 255 \text{ V}$$

$$(V_{\text{max}} - V_{\text{mean}}) / V_{\text{mean}} = 5 \% \quad (V_{\text{min}} - V_{\text{mean}}) / V_{\text{mean}} = - 2 \%$$

Calculations based on FEM-analysis regarding the effect of varying airgaps have been performed. Figure 27 shows how the flux linkage alternates when the airgap varies. In Figure 28 the relative flux linkage (relative to the flux linkage value when the airgap is 2mm) is illustrated. If we make the very simple assumption, regarding Figure 26, that the mean voltage (255 V) corresponds to an airgap of 2 mm, than it follows, comparing Figure 26 and Figure 28, that the maximum voltage (268 V, + 5 % rel mean value) corresponds to an airgap of about 1.8 mm and the minimum voltage (249 V, - 2 % rel mean value) corresponds to an airgap of about 2.1 mm. (This comparison between measured voltage and calculated flux linkage is of course relevant as we have a linearly dependence between flux linkage and induced voltage.)

The flux linkage variation (for small variations) is **approximately** linearly depending on the airgap variation. 5 % variation of the airgap results in about 5 % variation of the induced voltage and so on.

Voltage and 100*Current of the modules

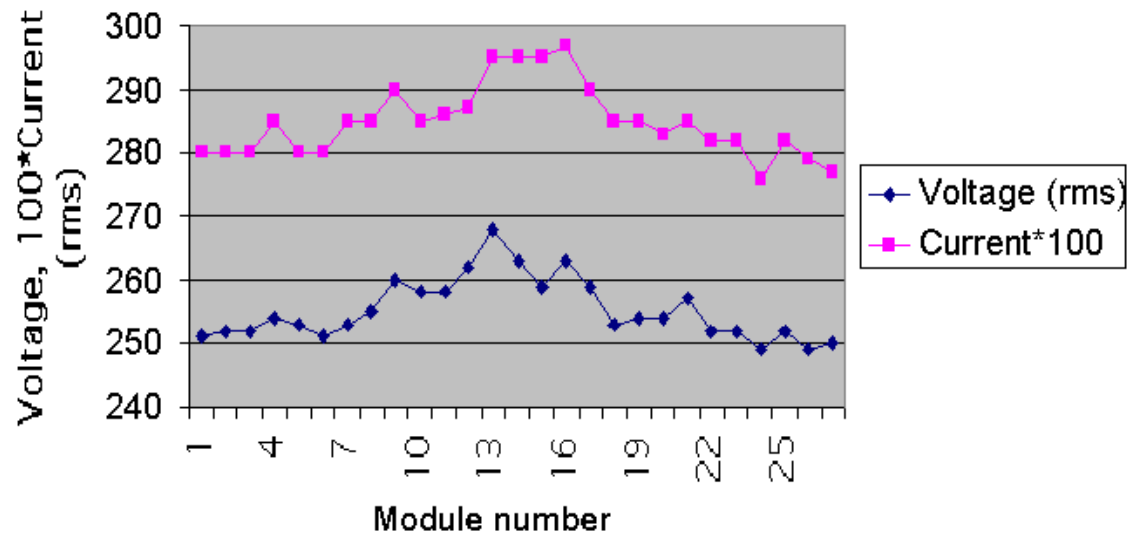


Figure 26 No load voltage and current of the modules

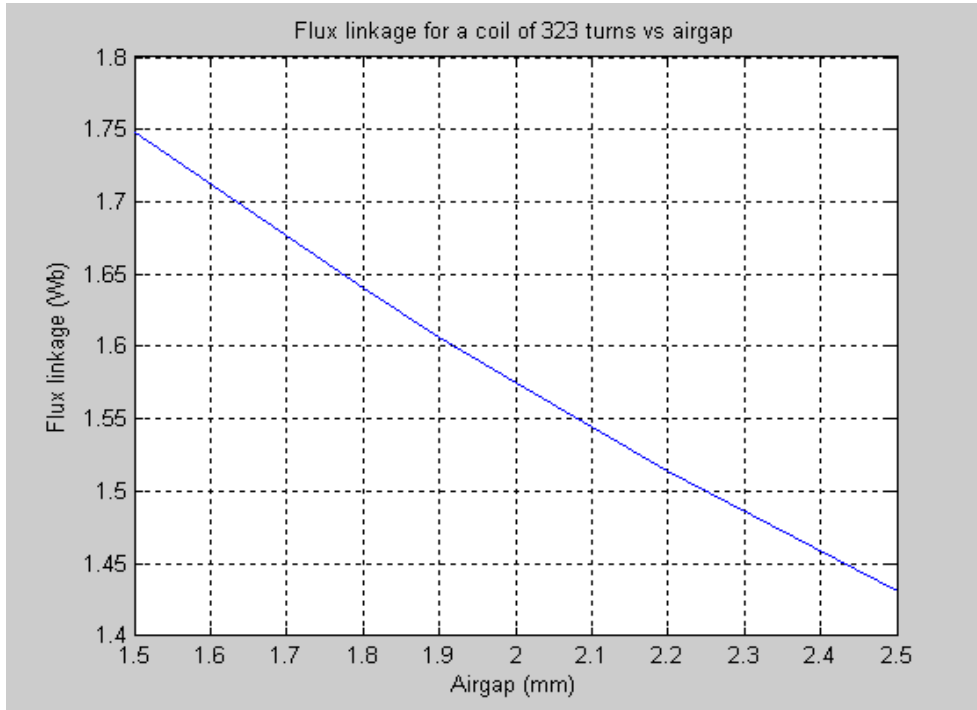


Figure 27 The resulted flux linkage (no current in the coil) vs airgap for a stator coil of 323 turns

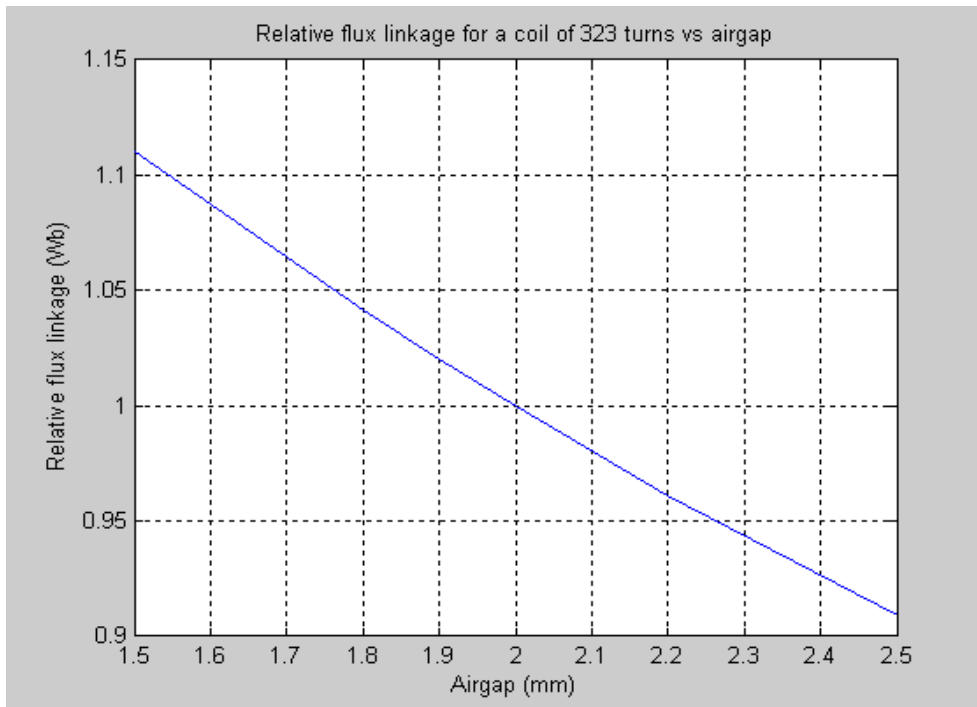


Figure 28 The relative flux linkage vs airgap. The reference is airgap = 2 mm

It is not only the induced voltage that is dependent on the airgap in question. Also the coil inductance will vary for alternating airgaps. Figure 29 illustrates the calculated coil inductance vs the airgap.

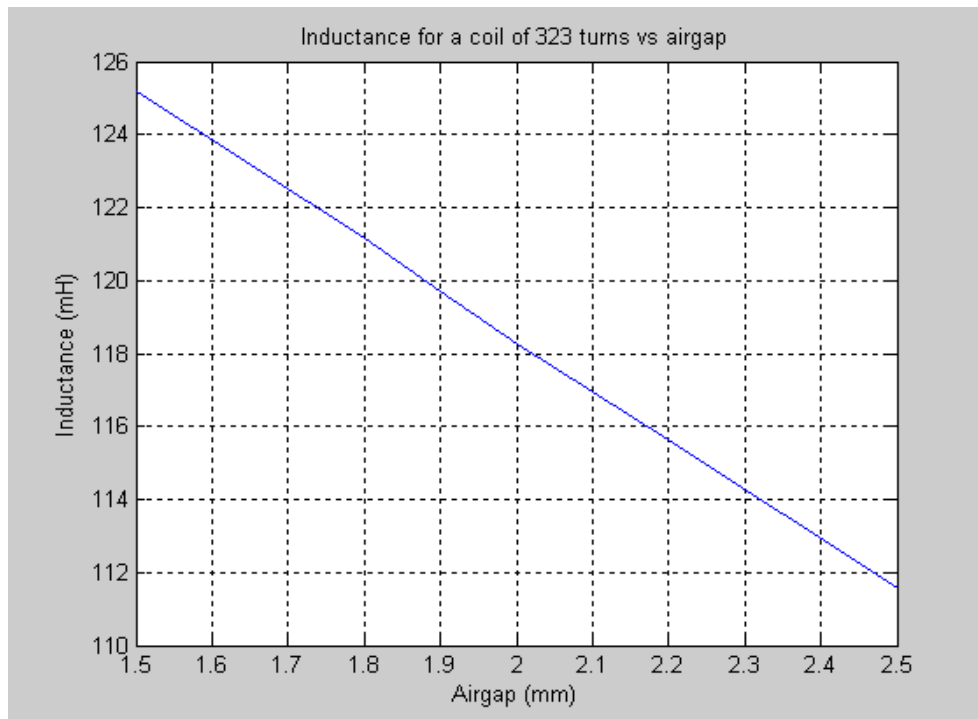


Figure 29 The coil inductance is dependent on the airgap

We have as a consequence of the discussion above two parameters, the induced voltage and the coil inductance, to take into account when analyzing the resulting effect of airgap variations. A future work that deal with this problem and that discuss the consequence on the power quality is recommended. See chapter 6.

5 FOURIER ANALYSIS REGARDING THE FLUX LINKAGE

5.1 General

A special kind of system analysis regarding the calculated flux linkage is realized by using the discrete calculated values as sample inputs to a discrete fourier analysis. Totally 66 calculated values give 66 sample points. The analysis results in a series of sine formed functions that together will modelle the flux linkage in question.

5.2 General about discrete fourier transforming

Suppose a continuous and real function $v(t)$ that is repeated with a periodic time T . This function could be divided into an infinite number of components according to:

$$(Equation 18) \quad v(t) = V_0 + \sum_{k=1}^{\infty} v_k(t)$$

$$(Equation 19) \quad v_k(t) = \sqrt{2}V_k \cos(k2\pi f_0 t + \phi_k)$$

$$(Equation 20) \quad V_k = \frac{\sqrt{2}}{T} \int_0^T v(t) \exp(-jk2\pi f_0 t) dt$$

$$(Equation 21) \quad V_0 = \frac{1}{T} \int_0^T v(t) dt$$

$$(Equation 22) \quad f_0 = \frac{1}{T}$$

Suppose a time dependent signal, e.g a voltage $v(t)$, that is sampled with N uniformed distributed samples in a measurement window T . Then we have the following time

points: $t_n = \frac{nT}{N}$, for $n = 0, 1, \dots, N-1$

If we transform the expression “ $V_k = \frac{\sqrt{2}}{T} \int_0^T v(t) \exp(-jk2\pi f_0 t) dt$ ” above into a discrete expression we get:

$$(Equation 23) \quad V_k = \frac{\sqrt{2}}{N} \sum_{n=0}^{N-1} v\left(\frac{nT}{N}\right) \exp(-j \frac{2\pi}{N} kn)$$

The so called discrete Fourier transform X is defined according to:

(Equation 24)
$$X_k = \sum_{n=0}^{N-1} x_n W_N^{kn}$$

x_n is the voltage value at time point n

(Equation 25)
$$W_N = \exp(-j \frac{2\pi}{N})$$

Return to the the voltage $v(t)$ and applying the defined discrete Fourier transform:

The DC-level:

(Equation 26)
$$V_0 = \frac{1}{N} X_0$$

The different harmonics:

(Equation 27)
$$V_k = \frac{\sqrt{2}}{N} X_k \quad k = 1, 2, \dots, N-1$$

The RMS values of the harmonics:

(Equation 28)
$$V_{k,RMS} = |V_k|$$

The phase angles of the harmonics:

(Equation 29)
$$\varphi_k = \arctan\left(\frac{\beta_k}{\alpha_k}\right)$$

where β_k is the **imaginary** part and α_k is the **real** part of V_k .

The frequency of the harmonics:

(Equation 30)
$$fm = \frac{m}{T} \quad m = 1, 2, 3, \dots, \frac{N}{2}$$

Appendix A 3 gives a "mat-lab"- program based on the expressions above.

5.3 D f t applied on the FEM result

Table 4 gives the calculated flux linkage values for a coil with 600 turns. The total shift interval corresponds to a total shift of one stator module. Figure 30 illustrates the flux linkage wave form for a coil with 323 turns when the rotor moves a shift of one stator module. Figure 31 illustrates the flux linkage vs time for a rotor speed of 80 rpm. As can be observed the wave form differs from a perfect sine curve. If we make a fourier analysis of the curve, using the program routine according to 0 (66 sample points corresponding to each calculated value are used) we get the result presented in

Table 5. As could be noted the fundamental (base) harmonic (e.g 32 Hz for a rotating speed of 80 rpm) is quite dominating. Figure 32 and Figure 33 illustrate the difference between the original calculated curve and the corresponding curve approximated with sine functions. In Figure 32 there is a comparison between the original calculated values and a sine function based on the fundamental frequency ($0.4 \cdot V_{rot} \cdot 1$, where V_{rot} : rotor speed (rpm)). As could be observed the flux function with a fair accuracy could be approximated with a single sine function. Figure 33 gives the corresponding result with 3 sine functions (1st , 3rd and 5th harmonics) taken into account. Here we can see that the two curves are very closed together.

Shiftposition (mm)	Flux linkage (Weber)	Shiftposition (mm)	Flux linkage (Weber)
0	-1.57463	85	1.550938
2.5	-1.56709	87.5	1.528867
5	-1.54017	90	1.489568
7.5	-1.49872	92.5	1.440042
10	-1.44704	95	1.381902
12.5	-1.38729	97.5	1.315687
15	-1.31946	100	1.245703
17.5	-1.25001	102.5	1.177873
20	-1.1811	105	1.108428
22.5	-1.11004	107.5	1.031985
25	-1.03145	110	0.944775
27.5	-0.93993	112.5	0.837647
30	-0.82634	115	0.705755
32.5	-0.68853	117.5	0.543717
35	-0.51895	120	0.350455
37.5	-0.32085	122.5	0.134045
40	-0.10013	125	-0.10013
42.5	0.134045	127.5	-0.32085
45	0.350455	130	-0.51895
47.5	0.543717	132.5	-0.68853
50	0.705755	135	-0.82634
52.5	0.837647	137.5	-0.93993
55	0.944775	140	-1.03145
57.5	1.031985	142.5	-1.11004
60	1.108428	145	-1.1811
62.5	1.177873	147.5	-1.25001
65	1.245703	150	-1.31946
67.5	1.315687	152.5	-1.38729
70	1.381902	155	-1.44704
72.5	1.440042	157.5	-1.49872
75	1.489568	160	-1.54017
77.5	1.528867	162.5	-1.56709
80	1.550938	165	-1.57463
82.5	1.555245		

Table 5 Calculated flux linkage as a function of shift position. No current in the coil

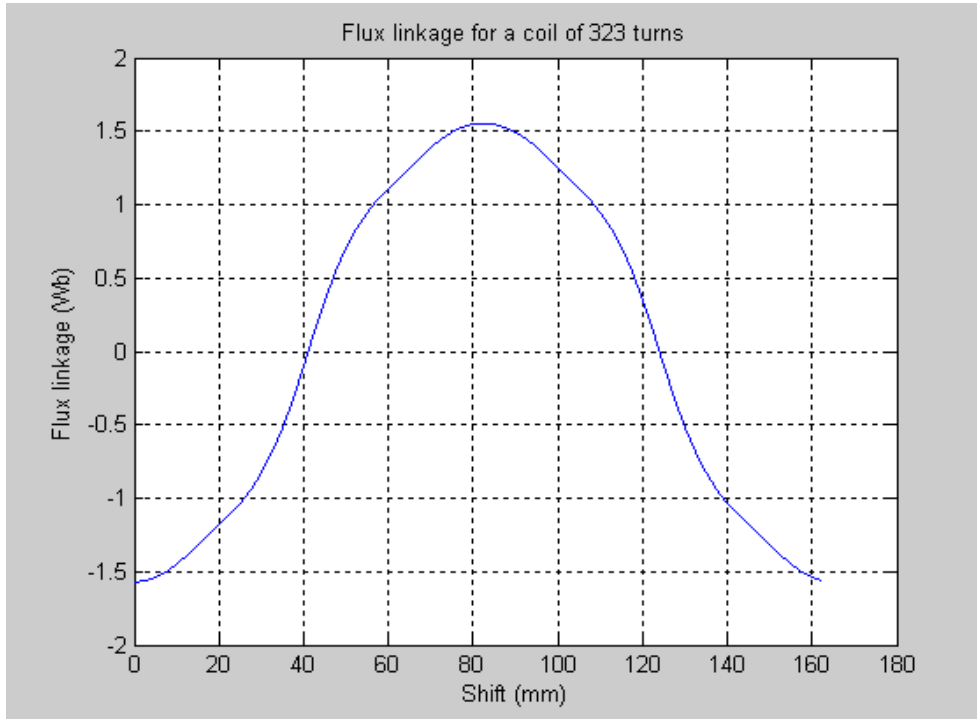


Figure 30 Flux linkage for a coil of 323 turns vs shift position. Total shift interval corresponds to one stator module.

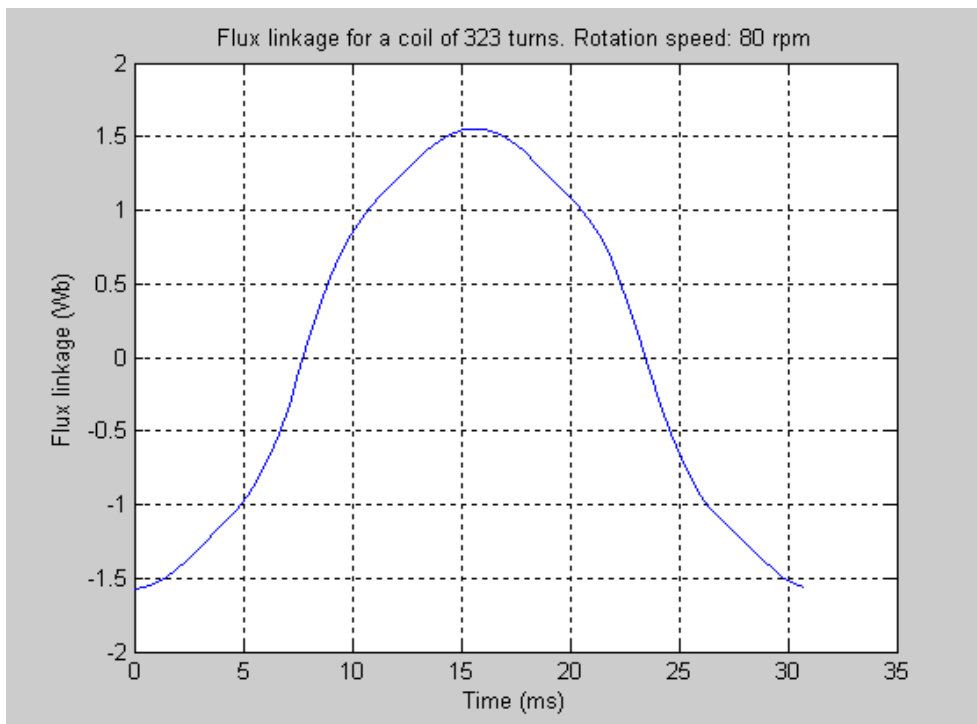


Figure 31 Flux linkage for a coil of 323 turns vs time. Rotation speed: 80 rpm

Parameter	Frequency (hz)	Amplitude (Wb)	Phase angle (rad)	Relation to 1 harmonic
Mean level	0	0.0015	-	0.1 %
1 harmonic (base)	$0.4 \cdot V_{rot} \cdot 1$	1.6166	π	1
2 harmonic	$0.4 \cdot V_{rot} \cdot 2$	0.0098	π	0.6 %
3 harmonic	$0.4 \cdot V_{rot} \cdot 3$	0.1076	0	6.7 %
4 harmonic	$0.4 \cdot V_{rot} \cdot 4$	0.0029	0	0.2 %
5 harmonic	$0.4 \cdot V_{rot} \cdot 5$	0.0696	π	4.3 %

Table 6 The result of fourieranalysis. V_{rot} : Rotor speed (rpm)

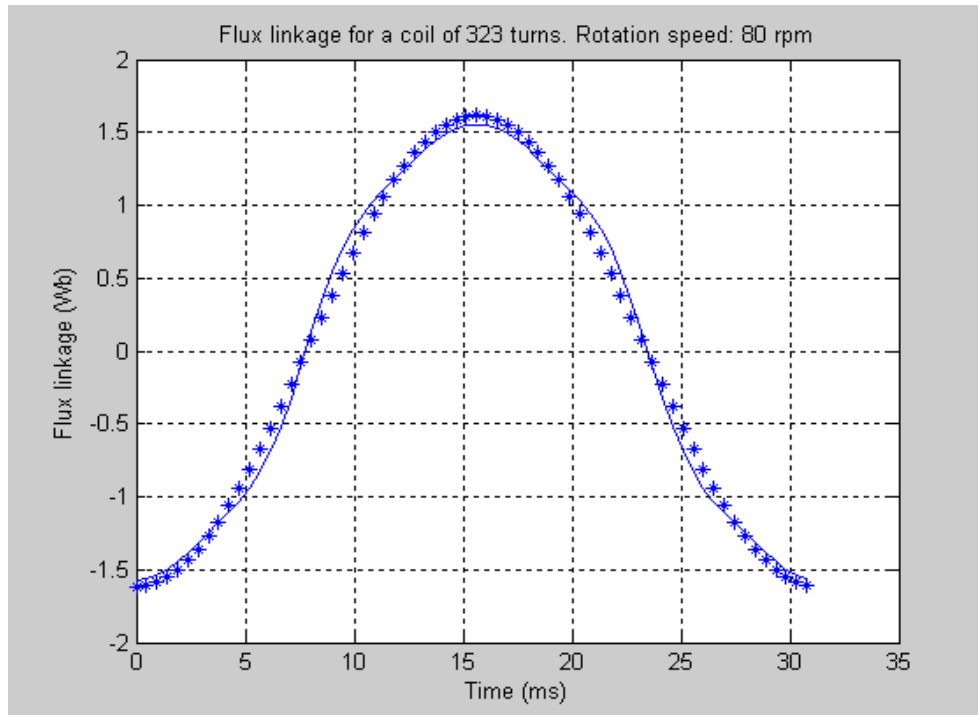


Figure 32 Flux linkage for a coil of 323 turns vs time. Rotation speed: 80 rpm
 — : original function ** : 1 sine function (1st harmonic)

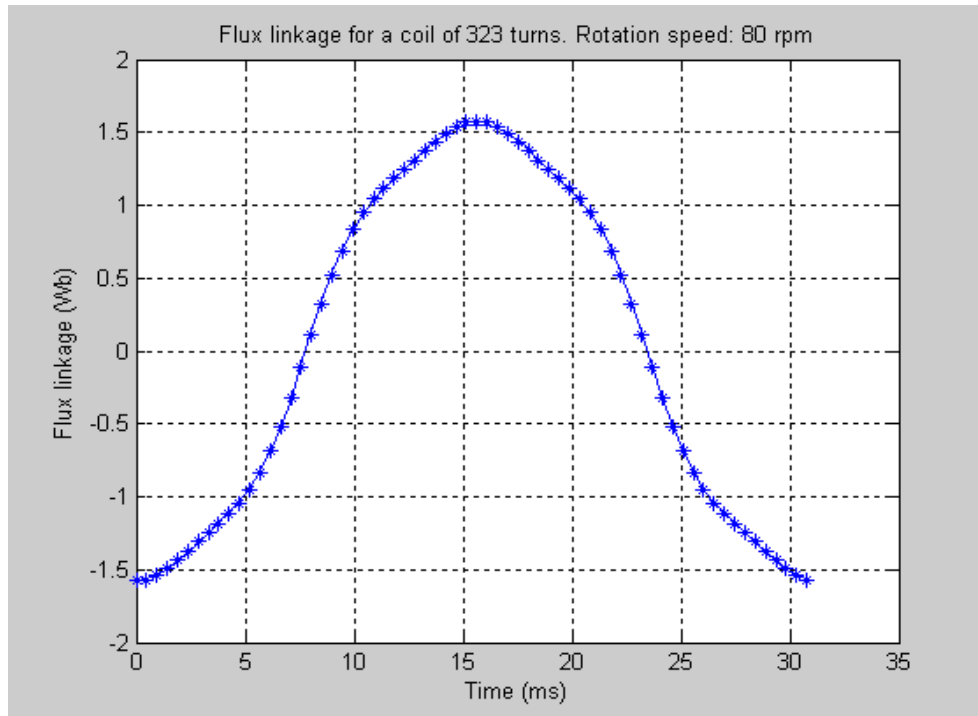


Figure 33 Flux linkage for a coil of 323 turns vs time. Rotation speed: 80 rpm
 — : original function ** : 3 sine functions (1st , 3rd and 5th harmonics)

5.4 Conclusion

According to the fourieranalysis of the calculated flux function the flux vs time could be described by using 3 sine functions with frequencies corresponding to 1st , 3rd and 5th harmonics:

$$\phi(t) = A_1 \cdot \cos(\omega_1 t + \alpha_1) + A_3 \cdot \cos(\omega_3 t + \alpha_3) + A_5 \cdot \cos(\omega_5 t + \alpha_5)$$

$$A_1 = 1.6166$$

$$A_3 = 0.1076$$

$$A_5 = 0.0696$$

$$\omega_1 = 2\pi \cdot 0.4 \cdot \Omega \cdot 1$$

$$\omega_3 = 2\pi \cdot 0.4 \cdot \Omega \cdot 3$$

$$\omega_5 = 2\pi \cdot 0.4 \cdot \Omega \cdot 5$$

$$\alpha_1 = \pi$$

$$\alpha_3 = 0$$

$$\alpha_5 = \pi$$

Ω = Rotor speed (rpm)

At this step we limit the description by using the first term.

i.e.: $\phi(t) = A_1 \cdot \cos(\omega_1 t + \alpha_1)$

As is illustrated in **Figure 32**, this results in a fair good approximation. However, in a future work, it could be of interest to more in detail investigate the contents of harmonics and its dependence of e.g mechanical design and the resulted effect on power quality. This is mentioned in chapter 6.

6 FUTURE WORK

The performed investigation of the Hönö generator has resulted in a number of interesting questions. The following ones are of immediate importance:

- The question regarding demagnetizing current. A more detailed study to define an appropriate upper current limit for the stator coils is recommended. See chapter 4.2.
- In the calculations according to chapter 4.1 we have regarded the coil inductance as independent of the stator-rotor relative position. However according to chapter 4.3 the inductance will vary as a function of relative position between stator pole and rotor pole. As the inductance has an influence on the resulting stator voltage, it could be a good idea to in the future, realize a more detailed analysis regarding the real effect of the inductance variation. Regarding the coil inductance we consequently have the following topics for coming studies:
 - complementary investigation of inductance distribution (measurements and calculations)
 - voltage dependent based on the inductance variations

7 REFERENCES

- [1] APPLIED COMPUTATIONAL ELECTROMAGNETICS
EXTRA PROJECT WORK
INVESTIGATION OF A GENERATOR MODEL
Chalmers, Juli 2003, Ingemar Mathiasson
- [2] Laboratory Measurements of a 40 kW Permanent Magnet
Generator
Chalmers, December 1998, Ola Carlson and Anders Grauers
- [3] Investigation of a Wind Power Generator. Part 2
Chalmers, Januari 2005, Ingemar Mathiasson

APPENDIX (USED SOFTWARE)

A 1 FEM-analysis

The FEM-calculations have been performed by a software named “Magnet” from Infolytica Corporation. The version of Magnet that have been used is limited to 2 dimensions and static calculations (2D Magnetostatic version).

A 2 Circuit Simulation

Circuit simulations have been performed by a software named “PLECS” ((Piecewise Linear Electrical Circuit Simulation). See chapter 4.1.

A 3 Discrete Fourier Calculations

A matlab-routine called "dft_1" has been used to perform discret fourier analysis. The base theory is described in chapter 5.2.

```
%
% Program dft_1
%
% Programmet genomför beräkning av den diskreta fouriertransformen för en samplad
signal
%
% Ingemar Mathiasson 6/6 - 04
%
%
% Den diskreta fouriertransformen beräknas enligt uttrycket:
%  $X(k+1)=DFT(X_n) = \sum_{n=0}^{N-1} x(n+1)W_N^{(k*n)}$ ,  $n=0,,$ , till  $N-1$ , där  $N$ 
% är antalet sampel inom mätfönstret
%  $W_N=\exp(-j*2*\pi/N)$ ;  $x(j)$ : samplad signal sampel  $j$ ;
% Följande gäller för den spektralanalyserade signalen: Medelnivå (likriktad
komponent):  $V_0 = 1/N * X(1)$ 
%
% RMS-värden för grundton och övertoner:  $V_k = \sqrt{2}/N * \text{abs}(X(k))$ ,  $k= 2, 3, \dots,$ 
 $N$ ,
% OBS! Det är endast de första  $N-1$  elementen som innebär ny information.
% Resten av elementen är en "spegling" map realaxeln
%
% Frekvenser:  $f(k) = 1/T, 2/T, \dots, N/2T$ 
%
```

```

% Fasvinklar:  $FI(k) = \arctan(b(k)/a(k))$ , där  $b(k)$  är imaginärdelen och  $a(k)$  är realdelen
an  $X(k)$ 

%

%

%

%

clear

%

% load s_fil % alternativ lagringsfil

%

% load s_fil_2 % alternativ lagringsfil

%

% load s_fil_flux_linkage % alternativ lagringsfil. Användes för lagring av
beräknade avlänkingsflöden. Antal spolvarv = 600

%

load s_fil_flux_linkage_2 % alternativ lagringsfil. Användes för lagring av
beräknade avlänkingsflöden. Antal spolvarv = 323

%

N=length (signal_s); % antal sampel

%

W_N=exp(-j*2*pi/N);

%

n_ton=6; % antal delkomponenter som skall analyseras (inkl DC-komponent)

%

for k=0:n_ton-1

%

```

```

Xk(k+1)=0;
%
for n=0:N-1
    x(n+1)=signal_s(n+1);
    Xk(k+1)=Xk(k+1)+x(n+1)*W_N^(k*n);
end
%
end
%
Xk(1)=Xk(1)/N;    % DC-komponent
for k=1:n_ton-1

Xk(k+1)=Xk(k+1)*sqrt(2)/N;

End

%
Xk_2=abs(Xk);    % ger sinussignalernas RMS-värden. Första elementet i vektorn
är DC-nivån

Xk_3=sqrt(2)*Xk_2; % ger sinussignalernas toppvärden. Första elementet i vektorn
är ej relevant

fas_vinkel=angle(Xk); % ger de olika komponenternas fasvinkel i radianer

%
%
% STOP

```